Angewandte Chemie
Eine Zeitschrift der Gesellschaft Deutscher Chemiker

Supporting Information



69451 Weinheim, Germany

# Identifying Enantiomers in Mixtures of Chiral Molecules with Broadband Microwave Spectroscopy**

*V. Alvin Shubert, David Schmitz, David Patterson, John M. Doyle, and Melanie Schnell**

anie_201306271_sm_miscellaneous_information.pdf

*- Supplementary material -*

***Content***



## *1. Experimental Details*

The Hamburg COMPACT spectrometer employed and modified for this study has been previously detailed elsewhere,[1] and thus only a brief overview of the experiment is given here, followed by a short description of the modifications made to perform this investigation. Figure 1B of the main article presents an overview schematic of the apparatus. The molecular samples of interest were heated in a sample holder and supersonically expanded into the vacuum chamber via pulse valves.

In broadband rotational spectroscopy, a microwave chirp spanning several GHz in only a few microseconds excites the molecules. An arbitrary waveform generator creates chirps that are amplified by a traveling wavetube amplifier and broadcast into the chamber with a horn antenna. When the molecules are resonant with a frequency within the chirp, a macroscopic polarization is created. The free induction decay (FID) of this polarization is recorded with a second microwave horn for up to 50 μs. In these experiments, 10 μs of the FID was recorded. The Fourier transform of this FID from the time to the frequency domain yields the microwave spectrum.

To perform the enantiomer-sensitive measurements of the chiral signal, the spectrometer was modified. We introduced a set of stainless steel electrodes as well as electronics for creating a radio frequency (RF) field in the interaction region between the broadcast and receiving horns. One electrode was connected to ground and the RF coupled to the second electrode via a coaxial cable. In addition, the broadcast horn was turned to 45° relative to the receiving horn as shown in Figure 1 of the main article. Note that this new experimental geometry provides both traditional MW spectra and chiral signatures with a single channel digitizer. However, due to this geometry, only the component of the signal linearly polarized along the longitudinal axis of the receiving horn can be recording. Thus, only half of the complete 3-wave mixing or traditional MW signal can be recorded with this arrangement. Ideally for 3-wave mixing, the receiving horn would be turned 90° relative to the excitation horn and for traditional MW signal it would be turned by 0°. In one set of experiments, two independently controlled pulsed valves were used.

Enantiomer-pure carvone (Sigma Aldrich, (R)-(-)-carvone (98%) or (S)-(+)-carvone (96%)) was used without further purification and heated to 120°C. For the initial three-wave mixing demonstration, a three-wave-mixing cycle with the greatest combined total predicted intensity p(total) = *p*(drive)**p*(twist)**p*(listen), where *p* is the predicted intensity of the transition)

was chosen and is illustrated in Figure 1 of the main article. The intensities were predicted with the rotational spectroscopy prediction program package SPCAT[2] using the rotational constants and MP2 calculated dipole moments from Moreno et al.[3] at a temperature of 1.0 K. The timing scheme for the microwave and radio frequency pulses is also shown in Figure 1 (main text). For this EQ2 three-wave mixing cycle, a 1 μs long and 60 MHz broad microwave chirp centered at the drive frequency was broadcast into the chamber. Overlapping temporally with the microwave chirp was the first 1 μs of the 5 μs long RF pulse. The single-frequency RF pulse has been optimized for the specific twist transition strength by adjusting the pulse duration.

Both the microwave chirp and RF pulse were generated on the same arbitrary waveform generator, which is a straightforward way to ensure phase stability. Inverting the original RF waveform shifted its phase by π radians. Changing the phase of the RF pulse by π radians by inverting the original RF waveform served as a useful diagnostic because it results in a reversed phase of the observed FID signal if it is due to three-wave mixing. Since we could generate the RF pulse (the "twist") with the second channel of our arbitrary waveform generator (while the output of the other channel was used for the microwave excitation chirp (the "drive")), the experiments required only one additional electronic component, namely an RF amplifier (50-550 MHz, 100 W, Kuhne electronics) to generate sufficiently strong RF pulses. The RF radiation was coupled into the vacuum chamber via double-ended BNC vacuum feedthroughs. The MW pulses were amplified with a 300W traveling wave tube amplifier.

**References**


[1] D. Schmitz, V. A. Shubert, T. Betz, M. Schnell, *J. Mol. Spectr*. **2012**, *280,* 77-84.

[2] H.M. Pickett, *J. Mol. Spectr*. **1991**, *148*, 371-377.

[3] J. R. A. Moreno, T. R. Huet, J. J. L. González, *Struct. Chem*. **2013**, *24*, 1163-1170.


## *2. Determination of the RF "twist" frequency*

For determining the RF "twist" frequencies used in the energy level cycles, we performed RF-MW double resonance experiments. This technique will be detailed in a forthcoming paper and is only briefly described in the following. We combined a microwave chirp of appropriate length (for example 2-6 GHz, 1 μs length for EQ1 of carvone) with a narrow RF pulse (500 ns). In the region of the predicted RF "twist" transition frequency, we scanned the frequency of the RF pulse in a step-wise manner with the same microwave excitation chirp at each step. To determine the twist frequency precisely, we measured both the phase and amplitude of the target microwave listen transition. As the RF frequency approaches resonance, first an increase in the magnitude of the phase occurs, followed by going through zero at the resonance, then the magnitude of the phase again increases, but with opposite sign. In a plot of the amplitude of the listen transition as a function of RF frequency, a depletion is observed as the RF resonance is approached, with a minimum at the RF resonance.

## *3. Determination of the Absolute Configuration*

The following variables are required for the discussion of the absolute configuration determination.

$\nu_i$ = frequency of listen transition for conformation *i*

$\phi_{eqi}^{E}$ = experimentally measured phase for conformation *eqi* from enantiomer *E*

$\phi_{abs}^{E}$ = absolute phase of enantiomer *E*

$N_{cyc}^{eqi}(t)$ = number of whole cycles within time *t* for conformation *eqi* at frequency $\nu_i$

$t_0$ = 0, time that excitation of conformation eq1 starts

$t_d$ = time that excitation of conformation eq2 starts

$t_r$ = time that recording of the FIDs starts

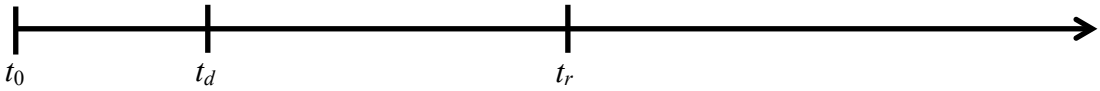


The phase of the 3-wave mixing signal measured experimentally can be computed if one knows the time between when the excitation occurred and the recording of the FID began and the absolute phase of the enantiomer, as shown in Equations 1-4.

$$\phi_{eq1}^{S} = 2\pi[\nu_1 t_r - N_{cyc}^{eq1}(t_r)] + \phi_{abs}^{S} \quad \text{Eq. 1}$$

$$\phi_{eq2}^{S} = 2\pi[\nu_2(t_r - t_d) - N_{cyc}^{eq2}(t_r - t_d)] + \phi_{abs}^{S} \quad \text{Eq. 2}$$

$$\phi_{eq1}^{R} = 2\pi[\nu_1 t_r - N_{cyc}^{eq1}(t_r)] + \phi_{abs}^{R} \quad \text{Eq. 3}$$

$$\phi_{eq2}^{R} = 2\pi[\nu_2(t_r - t_d) - N_{cyc}^{eq2}(t_r - t_d)] + \phi_{abs}^{R} \quad \text{Eq. 4}$$

In our experiment, $t_r$ is not known precisely enough to predict the phases. The reason is that there are delays in the electronics that must still be characterized. However, $t_d$ is well characterized, and we can thus solve for the predicted differences in the phases between the conformations, given in Equations 5 and 6.

$$\phi_{eq1}^{S} - \phi_{eq2}^{S} = 2\pi[t_r(\nu_1 - \nu_2) - \nu_2 t_d - N_{cyc}^{eq1}(t_r) + N_{cyc}^{eq2}(t_r - t_d)] \quad \text{Eq. 5}$$

$$\phi_{eq1}^{R} - \phi_{eq2}^{R} = 2\pi[t_r(\nu_1 - \nu_2) - \nu_2 t_d - N_{cyc}^{eq1}(t_r) + N_{cyc}^{eq2}(t_r - t_d)] \quad \text{Eq. 6}$$

Thus, one can solve Equations 5 and 6 over a range of times, $t_r$, and keep only those solutions that yield the measured phase differences. One can use these $t_r$'s and rearrange Equations 1-4 to predict the absolute phases with Equations 7-10.

$$\phi_{abs}^{S} = \phi_{eq1}^{S} - 2\pi[\nu_1 t_r - N_{cyc}^{eq1}(t_r)] \quad \text{Eq. 7}$$

$$\phi_{abs}^{S} = \phi_{eq2}^{S} - 2\pi[(\nu_2(t_r - t_d) - N_{cyc}^{eq2}(t_r - t_d)] \quad \text{Eq. 8}$$

$$\phi_{abs}^{R} = \phi_{eq1}^{R} - 2\pi[\nu_1 t_r - N_{cyc}^{eq1}(t_r)] \quad \text{Eq. 9}$$

$$\phi_{abs}^{R} = \phi_{eq2}^{R} - 2\pi[(\nu_2(t_r - t_d) - N_{cyc}^{eq2}(t_r - t_d)] \quad \text{Eq. 10}$$

Because the signs of the calculated dipole moment components are the same for both conformations, Equations 7 and 8 should give the same absolute phases, so only those solutions that do so are kept. The same condition is also true for Equations 9 and 10.

The last boundary condition is that the magnitude of the absolute phase should be identical for both enantiomers. And in fact, the magnitudes of the absolute phases should be equal to π/2. Although applying the condition $|\phi_{abs}^{S}| = |\phi_{abs}^{R}|$ to these solutions does not yield a unique value for $t_r$, the absolute phase for all solutions is the same. The recording time start is approximately $t_r$ = 6.7 μs, however a large range was chosen over which to compute the absolute phase, from 5.7-7.7 μs in 20

ps steps. Using the uncertainties in the observed phases to set the tolerances, 87 solutions for $t_r$ were found that match the conditions described above (comparing experimental vs. predicted phase differences between conformations, that the absolute phase is the same for both conformations of an enantiomer, and that the magnitude of the absolute phase is the same for both enantiomers). The absolute phases were $\phi_{abs}^{S} = -1.62(50)$ and $\phi_{abs}^{R} = 1.55(50)$ radians. The uncertainties were computed using a very conservative approach such that the true uncertainty is smaller than we report here.

The signal predicted from 3-wave mixing has the form:

$$sig(t) \propto \mu_a\mu_b\mu_c \cdot \sin(2\pi\upsilon t) \qquad \text{Eq. 11}$$

Or in a cosine basis:

$$sig(t) \propto \mu_a\mu_b\mu_c \cdot \cos\left(2\pi\upsilon t + \frac{\pi}{2}\right) \qquad \text{Eq. 12}$$

It is the phase of the signal that is the signature of the enantiomer, and since the dipole moment components, $\mu_{g=a,b,c}$ are signed quantities, Equation 13 can be rewritten as:

$$sig(t) \propto |\mu_a\mu_b\mu_c| \cdot \cos\left(2\pi\upsilon t + \frac{\mu_a\mu_b\mu_c}{|\mu_a\mu_b\mu_c|}\frac{\pi}{2}\right) \qquad \text{Eq. 13}$$

From DFT (B3LYP/aug-cc-pVDZ and B3LYP/aug-cc-pVTZ) calculations of the conformations and enantiomers of carvone, the signs of $\mu_a\mu_b\mu_c$ are -1 and +1 for S- and R-carvone, respectively. In the case of carvone, the sign does not depend on the two conformations seen in the supersonic expansion, a point implied earlier is assuming that the absolute phase is the same for both conformations. Thus, from Equation 13, the absolute phase in radians from S-carvone should be $\phi_{abs}^{S} = -\frac{\pi}{2} = -1.57$ and from R-carvone $\phi_{abs}^{R} = \frac{\pi}{2} = 1.57$. These predictions match very well with the absolute phases obtained experimentally, and the signs of the phases match exactly. These results need not be limited to this particular case because, in general, one could use the described combination of ab initio calculations, high-resolution microwave spectroscopy, and microwave three-wave mixing to determine the absolute configuration of even previously unidentified molecular samples from the experimentally obtained absolute phases.